



Investigation of ultraviolet radiation effects on thermomechanical properties and shape memory behaviour of styrene-based shape memory polymers and its composite

Wessam Al Azzawi^{a,b,*}, J.A. Epaarachchi^a, Jinsong Leng^c

^a Centre for Future Materials (CFM), Faculty of Health, Engineering and Sciences, University of Southern Queensland, Toowoomba, Queensland 4350, Australia

^b College of Engineering, Diyala University, Baqubah, Diyala, Iraq

^c Centre of Composite Materials and Structures, Harbin Institute of Technology (HIT), Harbin, China

ARTICLE INFO

Keywords:

SMP composites
Fixity and recovery behaviour
UV degradation

ABSTRACT

In recent years, shape memory polymers (SMP) have been researched extensively for space applications, such as deployable solar panels and antenna reflectors. Space applications cause SMP components to be severely exposed to ultraviolet (UV) light which may result in material degradation which may cause catastrophic failures and costs substantial amount of public money. This paper investigates the effect of UV light exposure on thermomechanical properties and shape memory effect (SME) of the Styrene-based SMP and its Glass fibre shape memory polymer composites (SMPC). Dynamic mechanical analysis (DMA) and thermogravimetric analysis (TGA), have been used to investigate the thermomechanical properties, SMEs and thermal stability before and after the UV exposure. Further, Fourier transform infrared spectroscopy (FTIR) was performed to analyse the after effect of UV exposure on the polymer's chemical structure. Results have revealed that UV exposure had different impacts on the SMP samples. UV exposure have degraded the mechanical properties, lowered the glass transition temperature (T_g), considerably reduced shape recovery rate, and programming and recovery stresses in all samples. However, the exposure had no considerable effect on the fixity ratio and relaxation modulus of the neat SMP sample, and it slightly increased the fixity ratio of the SMPC samples.

1. Introduction

The term “shape memory” denotes the aptitude of the materials to recover their original shape even though when it undergoes significant deformations. For a long time, shape memory alloys (SMAs) were the most well-known materials that exhibit this behaviour, however SMPs have emerged recently with excellent shape memory effect (SME) due to high flexibility of the polymer chains, and their unique microstructure architecture [1]. The common conventional SMP systems are cross-linked polyethylene Ota [2], polyethylene/nylon6 graft copolymers Li, Chen [3], styrene-based polymers Sakurai, Tanaka [4], and epoxy-based polymers [5].

The SME in SMPs is the result of the combination of polymer structure, polymer morphology, and the applied processing and activation technology. The proficiency of any SMP is strongly related to the polymers cross-linking which decide the material characteristics and the shape memory behaviour. The physically cross-linked,

Polyurethane-based SMP, for instance, has found to be less effective in SME compare to the chemically cross-linked SMPs [6]. In chemically cross-linked SMP, the crystalline phase with a crystal melting temperature (T_m) is used as a switch unit to provide the shape fixity effect Li, Chen [3], and to memorizes the permanent shape upon heating. Whereas physically cross linked SMPs have hard segment and soft segment; hard segment worked as pivoting point for shape recovery and soft segment could mainly absorb external stress applied to the polymer [7].

Most of polymers are impressionable to ultraviolet (UV), and show different types of degradation accordingly. Polymers, in general, absorb UV radiation chemically, and degrade as a result of energy accumulation over a long period of time [8]. Due to the combination of the photochemical effects with the hydrolytic effects of the environment, degradation in polymers could be severe Xu, Li [6], and the absorbed high-energy wavelengths of the UV spectrum may result in photo-oxidation effect [9]. The damaging effect of the UV exposure, for a specific

* Corresponding author. Centre for Future Materials (CFM), Faculty of Health, Engineering and Sciences, University of Southern Queensland, Toowoomba, Queensland 4350, Australia.

E-mail address: wessam.al-azzawi@usq.edu.au (W. Al Azzawi).

<https://doi.org/10.1016/j.compscitech.2018.07.001>

Received 3 April 2018; Received in revised form 30 June 2018; Accepted 1 July 2018

Available online 06 July 2018

0266-3538/ © 2018 Elsevier Ltd. All rights reserved.

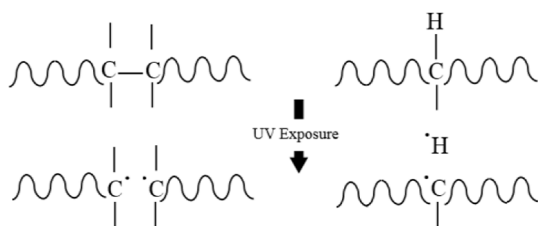


Fig. 1. Radicals initiation due to UV exposure.

polymer, depends on the bond types present. Energy required for the dissociation of the C–C and C–H bonds are 375 kJ/mol and 420 kJ/mol respectively which is equivalent to the UV radiation. Therefore, the UV photolysis and the polymers bond cleave effects are highly possible as a harmful effect of the exposure [9]. Thus, a radical is formed as a consequence of these reaction which in turn becomes a source for initiation of more radicals as shown in Fig. 1 [10].

However, the degradation in the polymers could range from minor visual effect (yellowing), to significant loss of mechanical properties, and change of molecular weight and molecular weight distribution [11–13].

Like other polymeric materials, SMPs may also undergo aging and degradation under UV radiation. Xie, Liu [14] have investigated the vacuum and UV radiation exposure effects on the cyanate-based SMP. Investigation results revealed that radiation has deepened the colour of the surface and shown some effects on the thermal stability of the SMP sample. Further, the irradiation induced some instability of the molecular structure within the material, and this effect was proportional to the increase of exposure time. However, results reported no significant change in the mechanical properties of the cyanate-based SMP. Further, both shape fixity rate and shape recovery rate were above 97.6% before and after UV radiation. Tandon, Goecke [15] have presented a study to assess the durability of styrene- and epoxy-based shape memory polymer resin materials when exposed to real life service environments, like water, oil, and UV light. The study observed the alterations in specimen colour, weight, and dimensions along with onset of damage due to conditioning. Moreover, parameters like rubbery and glassy phases' modulus, and shape memory behaviours, like stored strain, shape fixity, stress recovery ratio, and shape recovery were investigated under different environment conditions. Results demonstrated that UV exposure has resulted developing a yellow tint in both styrene- and epoxy-based SMPs, increased brittleness, and increased the average rubbery and glassy modulus of the styrene-based SMP specimens. A reduction in stress recovery ratio, due to the UV exposure was also reported in the study, however nil deterioration in the epoxy-based SMP, ability to store strain was observed, and almost complete recovery was possible after the UV exposure.

SMPs and their composites are of highly potential alternative material for aerospace and aircraft structural applications, such as reflectors, solar panels, and morphing wings [16] and [17]. Therefore, structural parts made of these material are expected to experience long term of UV light exposure. This type of harsh environment may significantly degrade the mechanical properties, the SME and even the service lifetime of SMPs and their SMPC [18].

In this paper, the effects of UV exposure on the thermomechanical properties and the SMEs of the styrene-based SMP and its glass fibre composite have been investigated. The exposure effects on material thermomechanical properties were investigated in terms of storage modulus and glass transition temperature. Whereas, the effects on the SMEs attitude were examined in terms of shape fixity, stress-free strain recovery, and constrained-strain stress recovery. Two groups of SMP and SMPC samples were prepared, and one of them was exposed to 1000 h of UV radiation in a UV chamber provided with air cooled Xenon arc [19]. A thermogravimetry analysis, and FTIR spectroscopy were performed to assess the irradiation effects on the material

chemical microstructure and thermal stability.

2. Materials and experimental techniques

2.1. Materials and samples preparations

Styrene-based SMP type C, which was supplied by Harbin Institute of Technology, China, has been used to manufacture the neat SMP and the SMPCs samples. The fibre used in the samples' manufacturing was woven glass fibre, AR177100 W/C 450 0/90, supplied by Colan Australia. A rectangular glass mould coated with thin film of Teflon was used to produce one neat SMP, and two different fibre fraction (20% and 25% SMPC) rectangular plates of $250 \times 200 \times 1.5 \text{ mm}^3$. After curing process in a temperature-controlled oven at 85°C for 24 h, prepared SMP and SMPC plates were divided into two groups, and one of the groups was exposed to UV irradiation in a UV chamber. After the UV irradiation, samples of the two groups were then cut into small specimens of $35 \times 14 \times 1.5 \text{ mm}^3$ according to the DMA Q800 single cantilever beam clamp standard. Three identical samples were prepared for each test type and the average of the results was calculated.

2.2. Experimental setup

A TA instruments dynamic mechanical analyser (DMA Q800) and thermogravimetry analyser (TGA Q500) have been used to investigate the specimens' thermomechanical properties and thermal stability. DMA was used in different operating modes, *DMA multi frequency-strain mode*, *DMA strain rate mode*, and *DMA Isostrain mode*. The first mode was used to examine the specimens' thermal and mechanical properties, while the second and third modes were used to conduct the specimens' programming and recovery tests. Recovery tests, in turn, were performed using two different methods, first method was programmed to characterize the shape fixity and stress-free strain recovery, whereas the second method was designed to investigate the constrained-strain stress recovery behaviour. Moreover, the TGA test was performed to investigate the thermal stability of the specimens. The test were implemented by heating the specimens, at constant rate, up to the material decomposition stage. During the test, specimens' weight was monitored as a function of temperature, and the decomposition temperature was located as the temperature corresponding to 5% drop in samples' original weight.

SUNTEST XLS equipment from ATLAS Material Testing Solutions shown in Fig. 2 was used to provide the UV light irradiance. The provided UV wavelength was in the range of 325–400 nm, and the UV intensity inside the chamber was 750 W/cm^2 . Samples were evenly distributed inside the chamber at equal distance from the UV source to assure similar exposure. The chamber was equipped with 2.2 kva air-cooled Xenon-lamp, and the exposure was done in an ambient atmosphere where the temperature was varied between 22 and 24°C , with a relative humidity between 30 and 50%.

FTIR equipment (IRAffinity-1S) fitted with signal reflection air accessory (GladiATR 10) from Shimadzu was used to conduct the spectroscopy measurement.

3. Testing procedures

3.1. Thermomechanical analysis tests

3.1.1. Glass transition temperature

Due to the significant difference between the material properties below and above T_g , careful investigation and precise determination of T_g is a vital starting point for any subsequent shape programming/recovery investigations. Above T_g , SMPs are in the rubbery state with low mechanical properties where shape programming can be done with minimum stress, however the glassy state, below T_g , makes the SMPs much stiffer. For T_g determination, DMA machine equipped with a



Fig. 2. SUNTEST XLS UV equipment, and schematic of the UV light chamber showing the components of the equipment 1. Specimens, 2. Sample table, 3. Xenon lamp, 4. Radiation, 5. Optical filter, 6. Mirror.

single cantilever beam bending clamp was used. The test was done using *DMA multi frequency-strain mode*, and the testing procedure involved temperature ramp at constant rate, 10 °C/min, up to 120 °C, and load was applied at a constant frequency of 1 Hz.

3.1.2. Shape programming

Shape programming process is the first stage of the of the SMPs' thermomechanical cycle. It starts by heating the material, which is in its permanent shape, to a temperature above T_g at a stress- and strain-free state. *DMA strain rate mode* was used with a custom procedure to do the shape programming process. The customised procedure was performed by going through a set of testing steps. First, *force* step with minimum value 0.001 N was set on the free end of the beam sample to ensure a proper contact between the sample and the machine movable clamp. Then, *temperature ramp* step was used to heat the sample up to 90 °C at a constant ramping rate of 5 °C/min. Thereafter, *isothermal* step was performed, for 3 min, to ensure a uniform temperature distribution inside the sample. After that, *ramp strain* step was implemented where 1.5% strain is applied with a strain rate of 0.5%/min. Subsequently, the sample was allowed to relax by *isothermal* step for 2 min, while it still at 90 °C and constant 1.5% strain. Then, compressed air at ambient temperature was used to cool down the sample from 90 °C to 35 °C, before the sample was freed from constrain, and programmed (temporary) shape was achieved.

3.1.3. Stress-free strain recovery

The stress-free recovery test is one of the main classical tests used to characterize the shape recovery properties of programmed SMPs samples. In our test, the DMA equipment was used with same operating mode as in shape programming stage, however the procedure settings are different. The procedure consisted the following steps; *force* step with 0.0 N was set first to ensure that the strain recovery occurs at a stress-free condition. Then, *temperature ramp* step was used to heat the sample from 35 °C to 85 °C with heating rate of 5 °C/min. Finally, an *isothermal* step was implemented at 85 °C for 40 min to allow the sample freely recover the original shape. It is important in this test to start the shape recovery test with the same strain value achieved at the end of the shape programming stage (stored strain), to assure the continuity of the strain value throughout the thermomechanical cycle.

3.1.4. Constrained-strain stress recovery

Constrained-strain recovery is the second class of the SMP recovery tests. It usually used to characterize the material capability to generate stress while it is recovering in isostrain condition. Similar to the unconstrained recovery test, this test should also starts with same stored strain value achieved by the end of the shape programming stage. However the difference here is strain value will be retained unchanged through the recovery process till the end. To do that, DMA equipment was used in a *DMA Isostrain mode*. This mode satisfies the condition of unchanged strain, through the test, by holding the movable part of the

DMA clamp fixed from the beginning till the end of the test. Further, test procedure was involved a *temperature ramp* step where samples were heated from 35 °C to 85 °C at 5 °C/min. Following, an *isothermal* step at 85 °C for 10 min was used to allow for uniform heating inside the sample, and give enough time for the sample to generate the recovery stress. Finally, the time history of the generated recovery stress and its associated heating process were reported.

3.2. Thermal stability

In thermogravimetry analysis, to evaluate the thermal stability, material is heated to elevated temperature and its decomposition is monitored by observing the samples' mass as a function of temperature. To investigate the thermal stability of the UV exposed and unexposed samples, a small specimens weight between (25–35 mg) have been cut out of the samples. They subjected to constant heating rate of 10 °C/min from room temperature to 650 °C while the weight versus temperature was monitored. The temperature at which specimens' weight dropped to 95%, was considered as decomposition temperature.

3.3. FTIR

In FTIR spectroscopy, the infrared radiation energy induces different molecular vibrational mods in the sample's covalent bonds. The produced spectrum represents the molecular fingerprint of the samples based on the percentage of the radiation absorbed or passed through the sample. Thin specimens of the exposed and unexposed SMP samples were used in a test spectrum range of 4000–600 cm^{-1} with scan times of 25 taking the air as reference. FTIR spectra in absorption mode was plotted against the wavenumber, and the peaks were characterised before and after the UV exposure to identify the UV exposure effects.

4. Results and discussions

The effects of UV light exposure on thermomechanical properties and SME of the styrene-based SMP and its glass fibre SMPC are illustrated in this section. UV degradation normally starts at the specimen outer surface, and then penetrates progressively into the bulk of the material [20]. Hence, Yellowing is the first indicator of the UV aging that can be easily visualized. Fig. 3 depicts the decolourization effect on the sample underwent the UV degradation, non-exposed sample was faded white while degraded one is dusky yellow.

4.1. Thermomechanical properties

4.1.1. Neat SMP

DMA results Figs. 4 and 5 demonstrate respectively the storage modulus and loss modulus of neat SMP samples before and after the exposure to UV light. It can be noticed that the exposure has significantly dropped the storage modulus at the glassy stage by

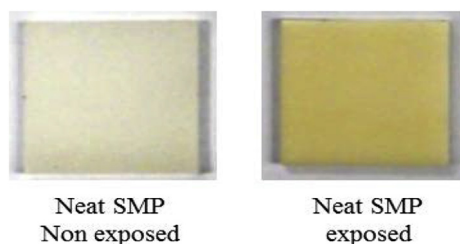


Fig. 3. Effect of 1000 h of UV exposure on the neat SMP sample colour. (For interpretation of the references to colour in this figure legend, the reader is referred to the Web version of this article.)

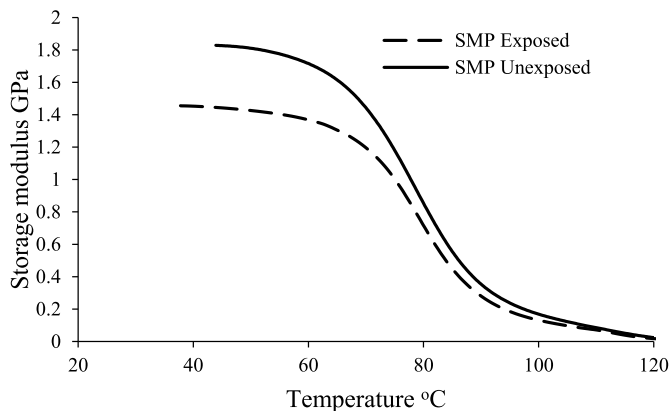


Fig. 4. Storage modulus vs temperature of neat styrene-based SMP exposed and unexposed to UV light.

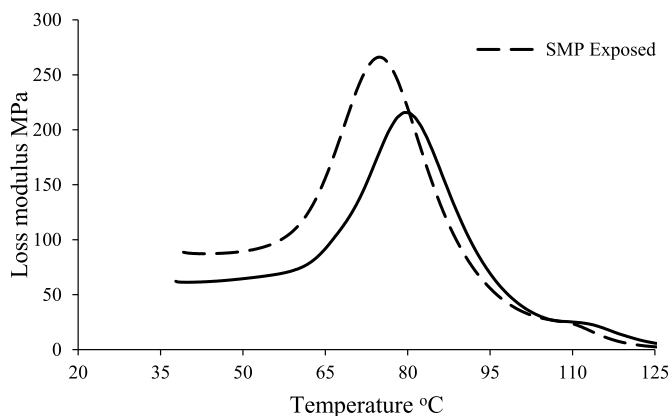


Fig. 5. Loss modulus vs temperature of neat styrene-based SMP exposed and unexposed to UV light.

approximately 25%, though the behaviour at the transition region and rubbery stages was closely identical to the behaviour of unexposed sample. Generally, UV degrades the polymers in two ways; exciting the electrons in the bonds between polymer chains, and producing thermal energy inside the polymers [8]. Therefore, the effect of UV degradation was more dominate at the glassy stage, because the polymer in this stage is at lower temperature, containing lower thermal energy, and consequently the electrons are more restricted compare to the rubbery stage.

Fig. 4 also depicts that, the UV exposure has reduced the difference between the storage modulus of the glassy and rubbery stages. This observation gives an important preliminary anticipation that UV exposure could worsen the SME because the bigger difference between the storage modulus of the glassy and rubbery phases is the better SME [21].

Moreover, Figs. 4 and 5 indicate that the UV exposure has changed

the glass transition temperature, the same behaviour was also reported recently by Ref. [14]. From Fig. 4, the onset of the storage modulus-temperature curve indicates the T_g which was found to be 70 °C and 66 °C for the unexposed and exposed samples respectively. Moreover, Fig. 5 depicts left shifting of the loss modulus curve of the exposed sample which also indicates a reduction in T_g from 79 °C to 75 °C.

TGA results in Fig. 6 illustrates the thermal gravimetric curves of neat SMP samples before and after the exposure to UV light. The two curves are perfectly overlapped over the temperature range from room temperature to approximately 375 °C. The initial decomposition temperature was considered as the temperature corresponding to 95% weight drop. For the unexposed and exposed samples, this temperature was 405 °C and 420 °C respectively. This indicates that UV exposure has improved in the SMP material thermal stability. The reason behind that could be due to the escape of the absorbed water and dioxide molecules from the unexposed sample during the exposure [14]. In general, the high decomposition temperature, above 400 °C, before and after the UV exposure, indicates good thermal stability of the Styrene-based SMP.

Fig. 7 depicts the transmittance FTIR spectra of the Styrene-based SMP before and after the exposure to UV light. As was shown in Fig. 3, the first effect of the UV exposure is the colour change. This effect has been started on the sample's surface and then gradually deepened as the UV irradiation increased [14]. This observation is confirmed in Fig. 7 where the UV exposure has changed the transmittance level which indicates a change of material colour to dusky. This is consistent with the earlier results reported by Ref. [22]. Furthermore, the IR spectra, before and after UV irradiation, indicates that most of the characteristic peaks at 696 cm^{-1} , 748 cm^{-1} and 1491 cm^{-1} remained steady. However, a new characteristic peak appeared at 1722 cm^{-1} which is corresponding to stretching vibration of the C=O bond. It is believed that the breaking of one end of the C–O bond, caused by the UV irradiation, was the reason of the newly created C=O bond [14]. This bond has higher energy which is leading to lower molecular weight of the system. As a part of UV exposure effects, molecular level changes may be implicated in the complex photo-chemical process which could induced property degradation, and weak bond breaking. Moreover, the characterised peak at 1722 cm^{-1} , due to the C=O double bond, indicates that the UV has degraded the methacrylate part. As a results, styrene was left alone in the material. Therefore, it is anticipated that UV exposure has changed the shape memory property of the material.

4.1.2. Fibre reinforced SMPCs

Fig. 8 illustrates the storage modulus curves of the neat SMP and the reinforced SMPC samples after the UV exposure. The results confirmed a development in storage modulus due to reinforcement. The percentage of development, relative to the exposed SMP sample, was 1 and 1.6 times for the 20% and 25% SMPCs respectively. However, Al Azzawi, Islam [23] have reported 1.75 and 2.35 times development in the modulus of the same SMPC unexposed samples. This denotes that UV exposure has resulted in 43% and 32% reduction in the modulus development envisaged from the reinforcement. The reason behind that could be the scission of the entanglements and tie chain molecules due to the exposure Popov, Blinov [24] which resulted in weaker engagement with the reinforcing fibres.

Furthermore, Fig. 9 shows the loss modulus curves of the 20% and 25% SMPC exposed samples where T_g was found to be 80 °C and 85 °C respectively compare to 75 °C for the exposed neat SMP reported in Fig. 5. This T_g increment attitude is conforming with the behaviour reported by Al Azzawi, Islam [23] for the unexposed samples. Therefore, it is realised that UV exposure has not changed the T_g increment tendency due to reinforcement even though it has reduced the T_g of the neat SMP sample shown in Fig. 4.

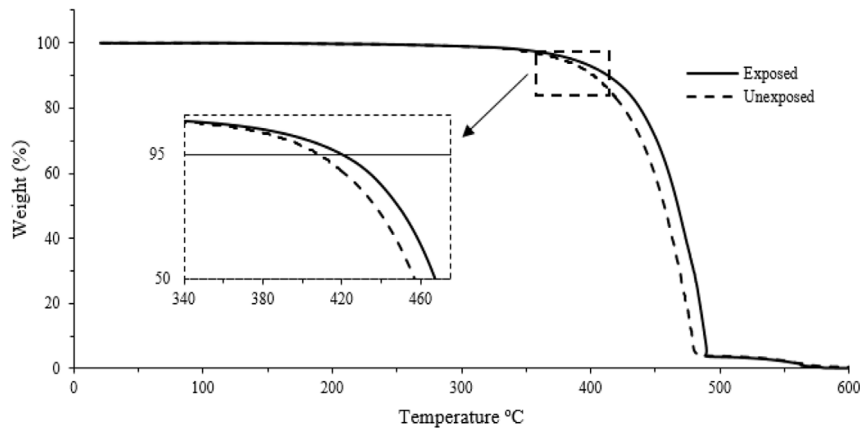


Fig. 6. Thermal gravimetric curves of the neat SMP samples exposed and unexposed to UV radiation.

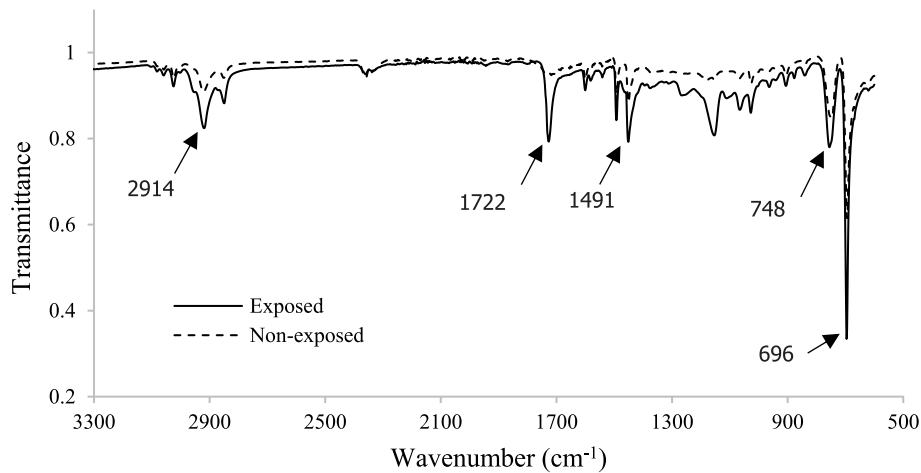


Fig. 7. FTIR spectra of the Styrene-based SMP exposed and unexposed to UV radiation.

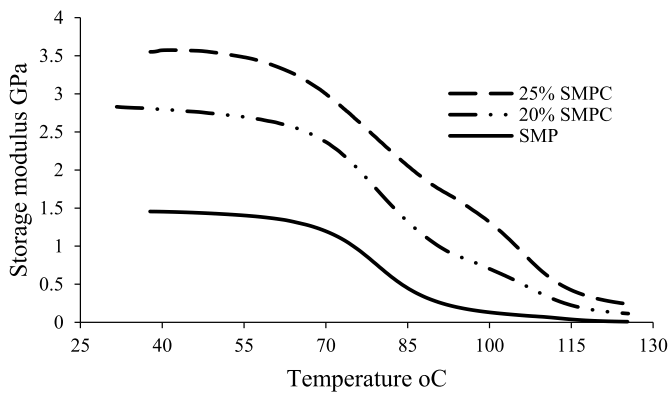


Fig. 8. Storage modulus-temperature relations of the UV exposed SMP, 20% and 25% SMPC samples.

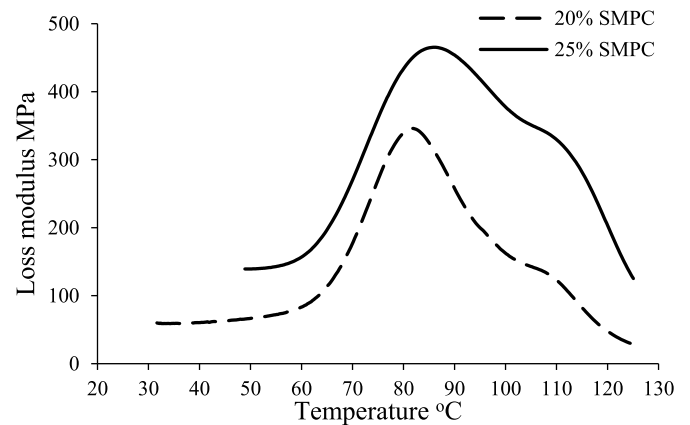


Fig. 9. Loss modulus-temperature relations of the UV exposed 20% and 25% SMPC samples.

4.2. Shape memory behaviour

4.2.1. Shape fixity and shape recover

Fig. 10 shows the effect of UV exposure on the shape memory behaviour of neat SMP and the SMPC samples. Both shape programming and stress-free shape recovery stages of the cycle are presented in addition to the associated heating and cooling steps.

Fig. 10 (a) presents the effect of the UV exposure on the neat SMP sample. Results show that UV exposure has negligible effect on the material capacity to hold the programmed temporary shape, as both exposed and unexposed samples have exhibited 98% shape fixity ratio.

This observation has conformed with observation reported in Ref. [14].

Fig. 10 (b and c) show that the shape fixity ratio of the 20% and 25% exposed SMPC samples has increased to 95% and 93% respectively compare to 93% and 91% in the unexposed SMPC samples. This improvement is attributed to the reduction in the SMPC spring back action resulted from the stiffness reduction due to the exposure.

Fig. 10 (a) also shows that the recovery process in the exposed and unexposed SMP samples has started almost simultaneously. This might be due to the relatively small difference in T_g between the two samples.

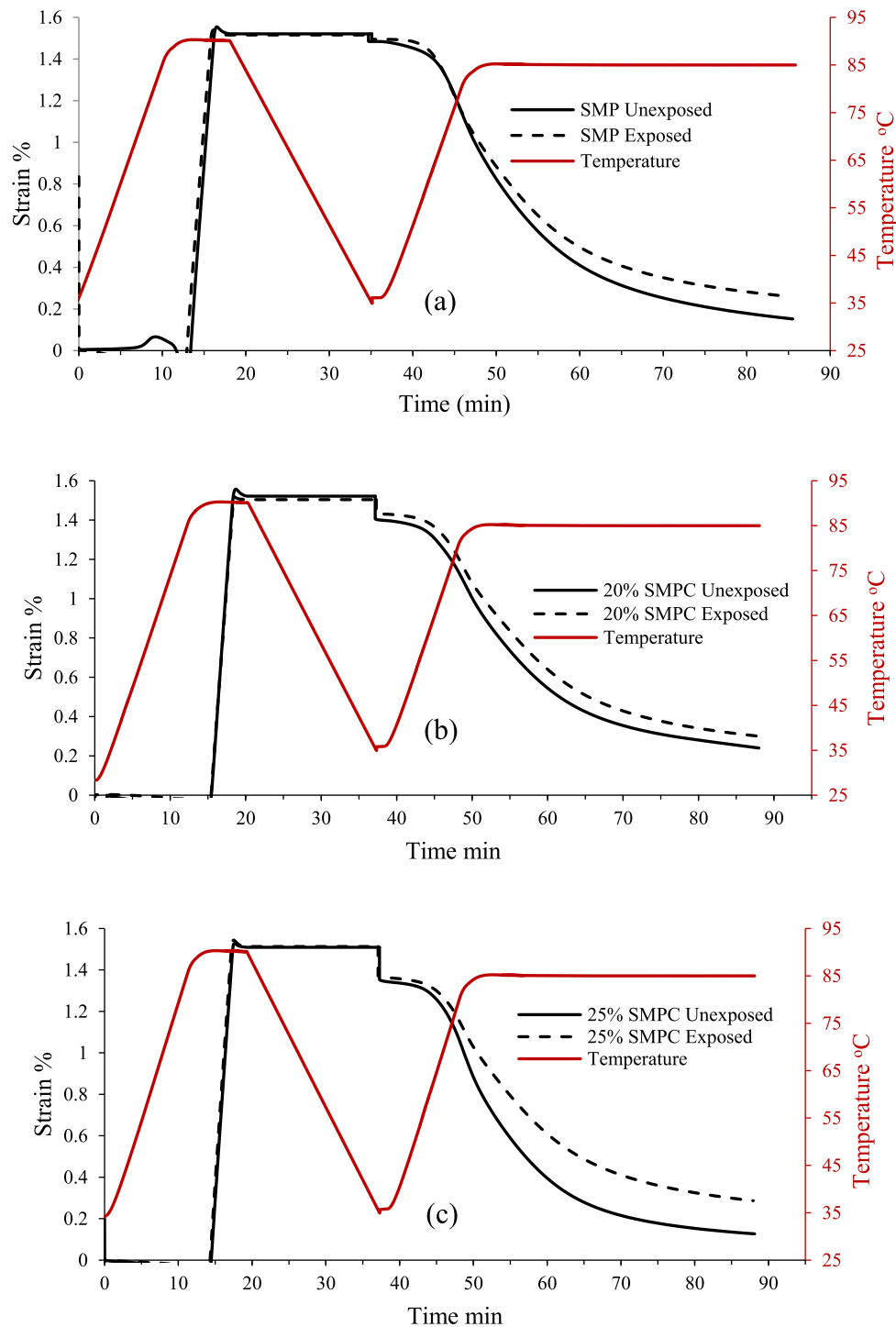


Fig. 10. Full thermomechanical cycle illustrating the shape programming and stress-free strain recovery processes and their associated heating and cooling steps for (a) neat SMP, (b) 20% SMPC and (c) 25% SMPC samples exposed and non-exposed to UV radiation.

Furthermore, shape recovery stage results have showed that exposed and unexposed samples have followed similar recovery behaviour at the beginning, then exposed sample has shown slower recovery at latter stages. The recovery has begun, in the SMP exposed and unexposed samples, at minute 35, and took 32 min and 40 min respectively to recover from stored strain to 0.3% strain. This indicates that exposure has resulted in 25% reduction in the recovery rate which might be because of the reduction in micro Brownian motion intensity caused by the UV radiation energy.

Fig. 10 (b) illustrates that the shape recovery process of the 20%

SMPC sample has commenced at the minute 37, and took 38 min and 51 min, for the unexposed and exposed samples respectively, to recover from the stored strain down to 0.3% strain. This indicates a 34% reduction in the sample's recovery rate because of the exposure. Similarly, Fig. 10 (c) shows that the shape recovery of the unexposed and exposed 25% SMPC sample has started at the minute 37, and took 27 min and 48 min respectively to recover from the stored strain to 0.3% strain which represent a 77% reduction. The different levels (25%, 34%, and 77%) of degradation in shape recovery rate between the SMP sample and the two SMPCs suggests that reinforcement fibre content has

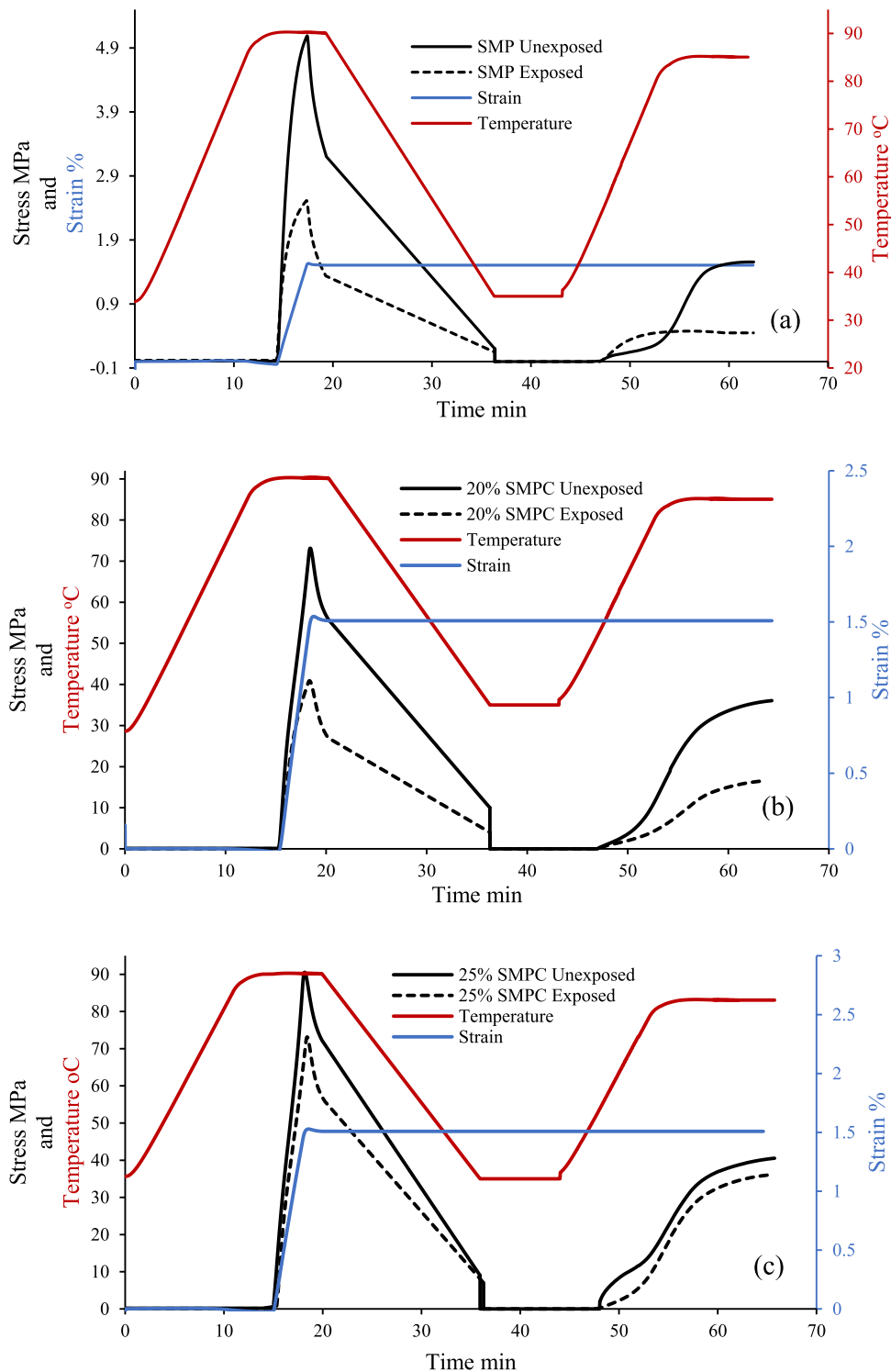


Fig. 11. Full thermomechanical cycle illustrating the shape programming stage, stress recovery stage, the associated heating/cooling stages, and the constrained strain for (a) neat SMP, (b) 20% SMPC and (c) 25% SMPC samples before and after the exposure to UV radiation.

altered the UV exposure effect on the material shape recovery behaviour. This can be ascribed to the extra reduction in micro Brownian motion intensity caused by the fibres, as a result, the molecule mobility and then the transformability from ordered configuration of the temporary shape to coiled configuration of permanent shape was reduced.

4.2.2. Stress recovery

Fig. 11 depicts the stress recovery behaviour under constrained

strain condition where the effects of the UV exposure on the stress developing ability of the sample were presented. Offered stress recovery cycle consists of two stages, shape programming stage which involves heating, deformation, cooling, and finally stress releasing step; and a stress recovery stage that includes a heating step only under a constrained strain condition. The strain achieved by the shape programming stage (1.5%) was kept constant throughout the stress recovery cycle.

Table 1

Programming and recovery stresses in the SMP and SMPC samples before and after the UV exposure.

Sample	Stress MPa		Stress reduction due to UV %	Stage
	Unexposed	Exposed		
SMP	5.6	2.4	57.1	Programming
20% SMPC	70.9	40	43.5	
25% SMPC	90	70.9	21.2	
SMP	1.5	0.44	70.6	Recovery
20% SMPC	36	27	25.0	
25% SMPC	40.5	35	13.5	

Fig. 11, shows that during the shape programming stages, material was heated up to 90 °C, then a specific stress was applied to develop the required programming strain (1.5%). It is observable that the programming stress of the unexposed samples was higher than that of the exposed samples. This is, indeed, anticipated behaviour owing to the material degradation caused by the UV exposure.

Fig. 11 (a, b, and c) show that in the shape programming stage, while the material at high temperature, programming stress has shown some drop before the starting of cooling step. This is because of the stress relaxation effect happens in the material which becomes dominant at higher temperature. This behaviour has been observed in all sample types, for both exposed and unexposed conditions. The percentage of stress relaxation in a particular sample was approximately equal before and after the exposure. This reflects a negligible effect for the UV exposure on the material's relaxation modulus.

Fig. 11 also elaborates a further stress drop stage starts simultaneously with the beginning of the cooling step. This drop is associated with the formation of the crystalline phase in the material as the temperature goes down. However, due to the stiffness of the crystalline phase, the stress in the material does not completely come to zero until the external stress release step is happened.

Fig. 11 also exhibit the stress recovery stage where stress emerges in the material as a consequence of temperature increase. Fig. 11 (a, b and c) shows that the exposed neat SMP sample has started developing recovery stress at almost 47 °C. However, for the exposed 20% and 25% SMPC samples the stress recovery has commenced at 51 °C and 54 °C respectively. This is attributed to the variation in T_g resulted from the fibre reinforcement discussed in Fig. 9.

Fig. 11(a–c) demonstrate that, during the recovery stage, stress was emerged from zero and developed progressively to its maximum as the temperature increased. The results revealed that the recovery stress in the exposed samples was lower than the unexposed samples. The reason behind this reduction is largely because of the degradation in material's modulus caused by exposure.

Table 1 provides the programming stresses and the recovery stresses in the SMP and SMPC samples before and after the UV exposure.

The results revealed that the exposure has reduced the SMP sample programming and recovery stresses by 57.1% and 70.6% respectively. However, for the SMPC samples, it looks that the reinforcement fibre has moderated the UV effect. As for the 20% and 25% SMPCs, the reduction in the programming and recovery stresses was considerably lower than the neat SMP sample.

5. Conclusion

The work presented here has intended to quantify the exposure effects due to UV light on the thermomechanical properties and the shape memory behaviour of Styrene-based SMP and its fibre composite. The investigations has considered the UV exposure effects on material modulus and glass transition temperature, shape fixity ratio, the stress-free strain recovery, and the constrained-strain stress recovery.

Results have shown that a yellowing in samples due to the UV aging,

and shown a reduction in the neat SMP samples' modulus and T_g . The TGA analysis performed on UV exposed samples has shown a 15 °C increase of the material decomposition temperature.

Stress-free strain recovery results have shown no significant effect of UV exposure on the shape fixity of the neat SMP sample. However, it has shown an improvement in the fixity ratio from 93% to 95% for the 20% SPMC, and from 91% to 93% for the 25% SMPC. Conversely, the exposure has reduced the shape recovery rate in the neat SMP, 20%, and 25% SMPC samples by 25%, 34% and 77% respectively. Moreover, the constrained-strain stress recovery test has revealed that UV exposure has reduced the programming stress by 57.1%, 43.5% and 21.2% in the SMP, 20% SMPC and 25% SMPC samples respectively. Further, it has significantly reduced the recovery stress, particularly in the neat SMP sample.

It can be concluded that, UV exposure has shown different impacts on the material properties of SMPC. As such further investigation of long-term behaviour of UV exposed SMP and SMPC are warranted in order to minimize unexpected failures.

References

- [1] A. Lendlein, S. Kelch, Shape-memory polymers, *Angew. Chem. Int. Ed.* 41 (12) (2002) 2034–2057.
- [2] S. Ota, Current status of irradiated heat-shrinkable tubing in Japan, *Radiat. Phys. Chem.* 18 (1–2) (1977) 81–87 1981.
- [3] F. Li, et al., Shape memory effect of polyethylene/nylon 6 graft copolymers, *Polymer* 39 (26) (1998) 6929–6934.
- [4] K. Sakurai, et al., Shape-memorizable styrene-butadiene block copolymer. I. Thermal and mechanical behaviors and structural change with deformation, *J. Macromol. Sci., Part B: Physics* 36 (6) (1997) 703–716.
- [5] T. Xie, I.A. Rousseau, Facile tailoring of thermal transition temperatures of epoxy shape memory polymers, *Polymer* 50 (8) (2009) 1852–1856.
- [6] T. Xu, G. Li, S.-S. Pang, Effects of ultraviolet radiation on morphology and thermo-mechanical properties of shape memory polymer based syntactic foam, *Compos. Appl. Sci. Manuf.* 42 (10) (2011) 1525–1533.
- [7] J. Hu, et al., Recent advances in shape-memory polymers: structure, mechanism, functionality, modeling and applications, *Prog. Polym. Sci.* 37 (12) (2012) 1720–1763.
- [8] T.-t. Wong, et al., Degradation of nano-ZnO particles filled styrene-based and epoxy-based SMPs under UVA exposure, *Compos. Struct.* 132 (2015) 1056–1064.
- [9] B. Singh, N. Sharma, Mechanistic implications of plastic degradation, *Polym. Degrad. Stabil.* 93 (3) (2008) 561–584.
- [10] V. Plotnikov, Effect of mechanical stresses on photochemical degradation of polymeric molecules, *Dokl Akad. Nauk SSSR*, 1988.
- [11] M. Abadal, et al., Study on photodegradation of injection moulded (beta)-polypropylene, *Polym. Degrad. Stabil.* 91 (3) (2006) p. 459e63.
- [12] A. Marek, et al., Spatial resolution of degradation in stabilized polystyrene and polypropylene plaques exposed to accelerated photodegradation or heat aging, *Polym. Degrad. Stabil.* 91 (3) (2006) 444–458.
- [13] J.W. Martin, J.W. Chin, T. Nguyen, Reciprocity law experiments in polymeric photodegradation: a critical review, *Prog. Org. Coating* 47 (3–4) (2003) 292–311.
- [14] F. Xie, et al., Effects of accelerated aging on thermal, mechanical and shape memory properties of cyanate-based shape memory polymer: I vacuum ultraviolet radiation, *Polym. Degrad. Stabil.* 138 (2017) 91–97.
- [15] G. Tandon, et al., Durability assessment of styrene-and epoxy-based shape-memory polymer resins, *J. Intell. Mater. Syst. Struct.* 20 (17) (2009) 2127–2143.
- [16] X. Lan, et al., Fiber reinforced shape-memory polymer composite and its application in a deployable hinge, *Smart Mater. Struct.* 18 (2) (2009) 024002.
- [17] X. Gong, et al., Variable stiffness corrugated composite structure with shape memory polymer for morphing skin applications, *Smart Mater. Struct.* 26 (3) (2017) 035052.
- [18] A. Fozza, et al., Oxidation and ablation of polymers by vacuum-UV radiation from low pressure plasmas, *Nucl. Instrum. Methods Phys. Res. Sect. B Beam Interact. Mater. Atoms* 131 (1–4) (1997) 205–210.
- [19] J. Rabek, *Polymer Photodegradation: Mechanisms and Experimental Methods*, Chapman Hall, New York, NY, 1995.
- [20] A. Blaga, *Deterioration mechanisms in weathering of plastic materials*, Durability of Building Materials and Components, ASTM International, 1980.
- [21] M. Fejős, G. Romhány, J. Karger-Kocsis, Shape memory characteristics of woven glass fibre fabric reinforced epoxy composite in flexure, *J. Reinforc. Plast. Compos.* (2012) p. 0731684412461541.
- [22] J. Pospišil, S. Nešpůrek, Photostabilization of coatings. Mechanisms and performance, *Prog. Polym. Sci.* 25 (9) (2000) 1261–1335.
- [23] W. Al Azzawi, et al., Quantitative and qualitative analyses of mechanical behavior and dimensional stability of styrene-based shape memory composites, *J. Intell. Mater. Syst. Struct.* (2017) p. 1045389X17705210.
- [24] A. Popov, et al., Oxidative destruction of polymers under stress, *Polym. Degrad. Stabil.* 7 (1) (1984) 33–39.